G. Sommer, N. Krüger, Ch. Perwass (Eds.): Mustererkennung 2000.
Springer, Berlin, pp. 460–467, 2000.

An Anisotropic Diffusion Algorithm with Optimized Rotation Invariance

Hanno Scharr[1] and Joachim Weickert[2]

[1] Interdisciplinary Center for Scientific Computing, Ruprecht Karls University, Im Neuenheimer Feld 368, 69120 Heidelberg, Germany
Hanno.Scharr@iwr.uni-heidelberg.de

[2] Computer Vision, Graphics, and Pattern Recognition Group, Dept. of Mathematics and Computer Science, University of Mannheim, 68131 Mannheim, Germany
Joachim.Weickert@ti.uni-mannheim.de

Abstract. For strongly directed anisotropic diffusion filtering it is crucial to use numerical schemes with highly accurate directional behaviour. To this end, we introduce a novel algorithm for coherence-enhancing anisotropic diffusion. It applies recently discovered differentiation filters with optimal rotation invariance [10], and comes down to an explicit scheme on a 5×5 stencil. By comparing it with several common algorithms we demonstrate its superior behaviour regarding rotation invariance and avoidance of blurring artifacts (dissipativity). We also show that the new scheme is more than three times more efficient than common explicit schemes on 3×3 stencils. It does not require to solve linear systems of equations, and it can be easily implemented in any dimension.

Keywords: Low-level vision, diffusion filtering, scale-spaces, rotation invariance, fast algorithms

1 Introduction

In this paper we present and evaluate a novel algorithm for coherence-enhancing anisotropic diffusion filtering. This scale-space and image restoration technique has been introduced for the enhancement of line-like structures [14]. The basic idea is to smooth an image by applying a diffusion process whose diffusion tensor allows anisotropic smoothing by acting mainly along the preferred direction. This so-called coherence orientation is determined by the structure tensor [3].

Since coherence-enhancing anisotropic diffusion filtering is essentially a one-dimensional smoothing strategy in a multidimensional image, it is of outmost importance to have a precise realization of the desired smoothing direction: for closing gaps in an interrupted line-like structure, for example, deviations from the correct smoothing direction will result in blurring artifacts. The main ingredient of our new algorithm is the consequent use of first-order derivative filters that have been optimized with respect to best gradient direction estimation [10]. We use these filters in an explicit (Euler forward) finite difference scheme. We will show that such an algorithm reveals better performance with respect to rotation invariance, creates less blurring artifacts and has more than three times higher efficiency than other explicit schemes. Moreover, the scheme is simple: it can be easily extended to higher dimensional data sets and it does not require to solve linear systems of equations.

The paper is organized as follows. In Section 2 we sketch the concept of coherence-enhancing diffusion filtering and review two common finite difference schemes. Section 3 presents our novel algorithm, followed by an experimental validation in Section 4. Finally we conclude with a summary in Section 5.

Related work. Although there is a rich literature on partial differential methods for image processing (see e.g. [4, 8]) the design of algorithms for anisotropic diffusion filters with a diffusion tensor has been addressed to a larger extend only recently. Numerical techniques include adaptive finite elements [9], and lattice Boltzmann techniques [5]. Explicit finite difference schemes [1, 2, 13] have been applied for simplicity reasons and semi-implicit stabilizations have been introduced to increase stability [14]. To the best of our knowledge, however, there is not a single publication that addresses the problem of designing algorithms for anisotropic diffusion filtering with an optimized directional behaviour.

2 Coherence-Enhancing Anisotropic Diffusion

2.1 General filter structure

Coherence-enhancing anisotropic diffusion filtering with a diffusion tensor evolves the initial image under an evolution equation of type

$$\frac{\partial u}{\partial t} = \nabla \cdot (D \nabla u)\,, \quad D = \begin{pmatrix} a & b \\ b & c \end{pmatrix} \tag{1}$$

where $u(x,t)$ is the evolving image, t denotes the diffusion time, and D is the diffusion tensor, a positive definite symmetric matrix that is adapted to the local image structure. This structure is measured by the structure tensor [3]

$$J_\rho(\nabla u_\sigma) = G_\rho * (\nabla u_\sigma \nabla u_\sigma^T) = \begin{pmatrix} J_{11} & J_{12} \\ J_{12} & J_{22} \end{pmatrix}.$$

The function G_ρ denotes a Gaussian with standard deviation ρ, and $u_\sigma := G_\sigma * u$ is a regularized version of u that is obtained by convolution with a Gaussian G_σ. The eigenvectors of J_ρ give the preferred local orientations, and the corresponding eigenvalues denote the local contrast along these directions. The structure tensor is highly robust under isotropic additive Gaussian noise [6]. The eigenvalues $\mu_1 \geq \mu_2$ of J_ρ are evaluated and the normalized first eigenvector can be written as $(\cos\alpha, \sin\alpha)^T$. The diffusion tensor D of coherence-enhancing anisotropic diffusion uses the same eigenvectors as the structure tensor, and its eigenvalues are assembled via

$$\lambda_1 := c_1\,, \qquad \lambda_2 := \begin{cases} c_1 & \text{if } \mu_1 = \mu_2, \\ c_1 + (1-c_1)\exp\left(\frac{-c_2}{(\mu_1-\mu_2)^2}\right) & \text{else,} \end{cases} \tag{2}$$

where $0 < c_1 \ll 1$ and $c_2 > 0$. The condition number of D is thus bounded by $1/c_1$, and the entries of D are given by

$$\begin{aligned} a &= \lambda_1 \cos^2\alpha + \lambda_2 \sin^2\alpha, \\ b &= (\lambda_1 - \lambda_2)\sin\alpha\cos\alpha, \\ c &= \lambda_1 \sin^2\alpha + \lambda_2 \cos^2\alpha\,. \end{aligned} \tag{3}$$

For more details on coherence-enhancing anisotropic diffusion we refer to [14].

2.2 Existing schemes

Equation (1) can be solved numerically using finite differences. Spatial derivatives are usually replaced by central differences, while the easiest way to discretize $\frac{\partial u}{\partial t}$ consists in using a forward difference approximation. The resulting so-called explicit scheme has the basic structure

$$\frac{u_{i,j}^{k+1} - u_{i,j}^{k}}{\tau} = A_{i,j}^{k} * u_{i,j}^{k} \quad \Leftrightarrow \quad u_{i,j}^{k+1} = (I + \tau A_{i,j}^{k}) * u_{i,j}^{k} \tag{4}$$

where τ is the time step size and $u_{i,j}^{k}$ denotes the approximation of $u(x,t)$ in the pixel (i,j) at time $k\tau$. The expression $A_{i,j}^{k} * u_{i,j}^{k}$ is a discretization of $\nabla \cdot (D\nabla u)$. It comes down to the convolution of the image with a spatially and temporally varying mask $A_{i,j}^{k}$. Hence, we may calculate u at level $k+1$ directly from u at level k via the right expression in (4).

The stencil notation of two common discretizations for $A_{i,j}^{k}$ are shown in Figure 1. We assume that the pixels have length 1 in both directions. The so-called standard discretization [13] from Fig. 1(a) is the simplest way to discretize Equation (1). It can be stabilized for larger time steps τ by a semi-implicit strategy using an additive operator splitting (AOS); see [14] for more details. The more complicated nonnegativity discretization from Fig. 1(b) offers the advantage of being absolutely stable if the condition number of the diffusion tensor does not exceed $3 + 2\sqrt{2} \approx 5.828$, and the time step size τ is sufficiently small [12]. This scheme has optimal rotation invariant behaviour within the class of 3×3 stencils [11], but Section 4 will show that its rotation invariance is not completely satisfying.

3 A Novel Algorithm with Optimized Isotropy

Let us now draw our attention to a novel algorithm, which is designed for better rotation invariance by using finite difference approximations on a 5×5 stencil. We rewrite the differential operator in (1) as

$$\nabla \cdot (D\nabla u) = \partial_x(a\partial_x u + b\partial_y u) + \partial_y(b\partial_x u + c\partial_y u). \tag{5}$$

a

$\frac{b_{i-1,j}-b_{i,j+1}}{4}$	$\frac{c_{i,j+1}+c_{i,j}}{2}$	$\frac{b_{i+1,j}+b_{i,j+1}}{4}$
$\frac{a_{i-1,j}+a_{i,j}}{2}$	$-\frac{a_{i-1,j}+2a_{i,j}+a_{i+1,j}}{2}-\frac{c_{i,j-1}+2c_{i,j}+c_{i,j+1}}{2}$	$\frac{a_{i+1,j}+a_{i,j}}{2}$
$\frac{b_{i-1,j}+b_{i,j-1}}{4}$	$\frac{c_{i,j-1}+c_{i,j}}{2}$	$\frac{b_{i+1,j}-b_{i,j-1}}{4}$

b

$\frac{\lvert b_{i-1,j+1}\rvert-b_{i-1,j+1}}{4}+\frac{\lvert b_{i,j}\rvert-b_{i,j}}{4}$	$\frac{c_{i,j+1}+c_{i,j}}{2}-\frac{\lvert b_{i,j+1}\rvert+\lvert b_{i,j}\rvert}{2}$	$\frac{\lvert b_{i+1,j+1}\rvert+b_{i+1,j+1}}{4}+\frac{\lvert b_{i,j}\rvert+b_{i,j}}{4}$
$\frac{a_{i-1,j}+a_{i,j}}{2}-\frac{\lvert b_{i-1,j}\rvert+\lvert b_{i,j}\rvert}{2}$	$-\frac{a_{i-1,j}+2a_{i,j}+a_{i+1,j}}{2}-\frac{\lvert b_{i-1,j+1}\rvert-b_{i-1,j+1}+\lvert b_{i+1,j+1}\rvert+b_{i+1,j+1}}{4}-\frac{\lvert b_{i-1,j-1}\rvert+b_{i-1,j-1}+\lvert b_{i+1,j-1}\rvert-b_{i+1,j-1}}{4}+\frac{\lvert b_{i-1,j}\rvert+\lvert b_{i+1,j}\rvert+\lvert b_{i,j-1}\rvert+\lvert b_{i,j+1}\rvert+2\lvert b_{i,j}\rvert}{2}-\frac{c_{i,j-1}+2c_{i,j}+c_{i,j+1}}{2}$	$\frac{a_{i+1,j}+a_{i,j}}{2}-\frac{\lvert b_{i+1,j}\rvert+\lvert b_{i,j}\rvert}{2}$
$\frac{\lvert b_{i-1,j-1}\rvert+b_{i-1,j-1}}{4}+\frac{\lvert b_{i,j}\rvert+b_{i,j}}{4}$	$\frac{c_{i,j-1}+c_{i,j}}{2}-\frac{\lvert b_{i,j-1}\rvert+\lvert b_{i,j}\rvert}{2}$	$\frac{\lvert b_{i+1,j-1}\rvert-b_{i+1,j-1}}{4}+\frac{\lvert b_{i,j}\rvert-b_{i,j}}{4}$

Fig. 1. **a** Standard [13] and **b** nonnegativity discretization [12]

This expression is now evaluated in an explicit way, i.e. using only known values from the old time level k. The key point is the usage of first order derivative operators with the stencil notations

$$F_x = \frac{1}{32}\begin{bmatrix} -3 & 0 & 3 \\ -10 & 0 & 10 \\ -3 & 0 & 3 \end{bmatrix} \quad \text{and} \quad F_y = \frac{1}{32}\begin{bmatrix} 3 & 10 & 3 \\ 0 & 0 & 0 \\ -3 & -10 & -3 \end{bmatrix}. \tag{6}$$

These filters have been derived recently in [10, 7], where the goal was to optimize rotation invariance. They improve direction estimation by more than 3 orders of magnitude, compared to related popular stencils like the Sobel filters. As each filter is separable and contains only two different numbers, convolution is cheap (2 multiplications, 2 additions due to separability, 1 subtraction per pixel).

Now we proceed in four steps, where derivatives are always computed using the optimized derivative filters from (6):

1. Calculate the structure and diffusion tensor.
2. Calculate the flux components $j_1 := a\partial_x u + b\partial_y u$ and $j_2 := b\partial_x u + c\partial_y u$.
3. Calculate $\nabla \cdot (D\nabla u) = \partial_x j_1 + \partial_y j_2$.
4. Update in an explicit way.

Since the resulting scheme makes consequent use of the optimized derivative filters, we may expect good directional behaviour. The total stencil of this scheme

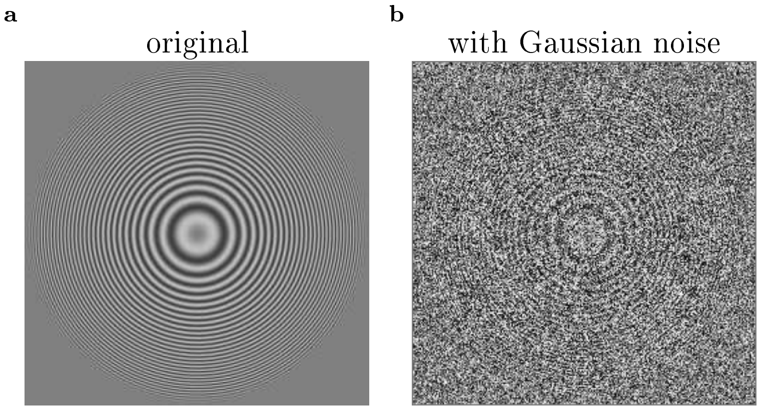

Fig. 2. Test image: **a** Original, **b** with Gaussian noise.

has size 5×5, since we are approaching the second order derivatives by consecutively applying first order derivatives of size 3×3. We refrain from writing down the resulting stencil, since it is nowhere needed in the entire algorithm.

4 Experimental Validation

4.1 Rotation invariance and dissipativity

Tests were performed on a ring image with varying frequencies (see Figure 2(a)). Its maximum wave number is 0.5 . We consider three different explicit diffusion schemes: the standard scheme, the nonnegativity scheme and our novel one. We apply 100 iterations with $c_1 := 0.001$, $c_2 := 1$, $\sigma = 0.001$, $\rho = 1.0$, $\tau = 0.2$. Applying diffusion with these parameters to the ring image should not deteriorate the rotation invariance. It should be altered only by some small amount of isotropic diffusion caused by the parameter c_1 (for analytical results see [11]). Figure 3 shows the results for the upper right quadrant. The other quadrants look similar. For small wave numbers, all schemes perform well. For larger wave numbers, however, the standard scheme introduces severe blurring artifacts for all directions except for the directions of the coordinate axes. The nonnegativity discretization shows similar dissipative effects. However, it also performs well along the grid diagonals. For the new scheme dissipative effects or deviations from rotational invariance cannot be observed. To demonstrate the importance of rotation invariance, we apply our three implementations in order to reduce Gaussian noise that has been added to the test image (cf. Fig. 2(b)). The Gaussian noise has zero mean, and the standard deviation has the same magnitude as the signal amplitude. Figure 4 shows the upper right quadrant using the same parameters as before. Only the new scheme reconstructs the signal satisfactory for all orientations and frequencies.

a original **b** standard scheme **c** nonneg. scheme **d** new scheme

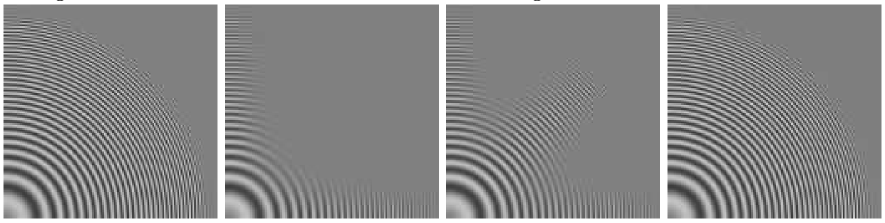

Fig. 3. Rotation invariance and dissipativity test: the upper right quadrant of the ring image after applying three schemes for coherence-enhancing diffusion filtering.

a original **b** standard scheme **c** nonneg. scheme **d** new scheme

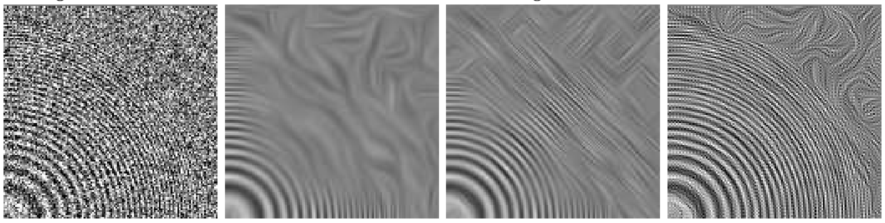

Fig. 4. Restoration of the upper right quadrant of the noisy ring image from Fig. 2(b).

In order to demonstrate that directional errors should not be neglected for real data either, we applied the three algorithms to a 206×160 image of a peacock. The general impression from Figure 5 is that the new scheme produces the sharpest and most detailed results. As in Fig. 3 the standard and nonnegativity schemes show blurring artifacts for nongrid directions.

4.2 Efficiency and stability

Let us now evaluate the efficiency of our method in comparison with explicit standard and nonnegativity discretizations, and an AOS-stabilized semi-implicit standard discretization [13]. We did not display results for the latter scheme in the previous experiments, because they were visually identical with those from the underlying explicit standard discretization.

The total efficiency of an iterative method is the product of the computational cost for one iteration and the number of iterations that are required for reaching a fixed diffusion time T. The iteration number depends on the largest time step size under which the scheme is stable. Unfortunately, no theoretical stability bounds are available, since neither the von Neumann stability using the Fourier transform nor stability reasonings based on maximum–minimum principles can be applied.

Therefore, we have to perform experimental stability measurements. As a stability criterion we use the temporal evolution of the variance of the filtered image, which has to decrease monotonically [12]. Thus, if the variance is increased

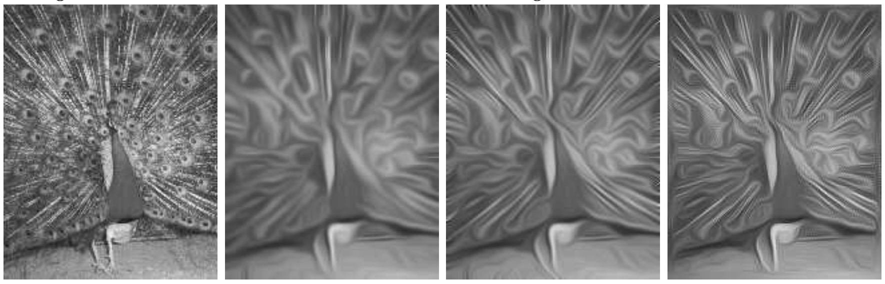

Fig. 5. Dissipativity illustrated by means of a 206 × 160 image of a peacock. The filter parameters are $c_1 = 0.001$, $c_2 = 1$, $\sigma = 0.6$, $\rho = 2$, $\tau = 0.2$, and 100 iterations.

Table 1. Efficiency of the different methods on a PC (Pentium III, 700 MHz). All algorithms were implemented in a comparable way using ANSI C, and we used the peacock image and the filter parameters from Fig. 5.

discretization	CPU time t_{CPU} per iteration	stability bound τ_{max}	recommended step size τ	efficiency τ/t_{CPU} $[s^{-1}]$
explicit, standard	0.0906 s	0.5	0.25	2.76
explicit, nonnegativity	0.0938 s	0.5	0.25	2.67
AOS-stabilized, standard	0.0996 s	2.1	1.0	10.04
new scheme	0.1093 s	2.1	1.0	9.15

from one step to the next, it is a clear sign of instabilities. As an upper estimate for an experimentally stable behaviour we have searched for the largest time step size for which the variance decreases monotonically.

The results of our efficiency analysis are depicted in Table 1. These stability bounds are overestimated, as instabilities may arise before the monotony of the variance is violated. To be on the safe side we recommend to use time step size 0.25 for the explicit standard or nonnegativity schemes, and step size 1 for the AOS-stabilized and our novel scheme. This shows that our novel scheme is not only accurate, but also quite efficient: it is almost as fast as the semi-implicit AOS-stabilized scheme and more than three times more efficient than the other explicit techniques. For further information on stability, quantitative errors and possible modifications of the new algorithm we refer to [11, 15].

5 Summary and Conclusions

We have introduced an explicit discretization for coherence-enhancing anisotropic diffusion filtering that uses optimized first-order derivative approximations. In a comparison with existing schemes we have shown its superior directional performance. This point is very important for anisotropic diffusion techniques, since directional errors introduce visible smoothing artifacts. We have also shown that our scheme, which comes down to averaging over 5×5 masks, allows to use four times larger time step sizes than conventional explicit schemes that perform 3×3 averaging. With this efficiency gain it is almost as efficient as an AOS-stabilized semi-implicit technique. These performance characteristics render it appealing in all situations where a simple anisotropic diffusion algorithm is needed that combines good quality with high efficiency.

References

1. G.-H. Cottet, M. El Ayyadi, *A Volterra type model for image processing*, IEEE Trans. Image Proc., Vol. 7, 292–303, 1998.
2. G.-H. Cottet, L. Germain, *Image processing through reaction combined with nonlinear diffusion*, Math. Comp., Vol. 61, 659–673, 1993.
3. W. Förstner, E. Gülch, *A fast operator for detection and precise location of distinct points, corners and centres of circular features*, Proc. ISPRS Intercommission Conf. on Fast Processing of Photogrammetric Data (Interlaken, June 2–4, 1987), 281–305, 1987.
4. B. ter Haar Romeny, L. Florack, J. Koenderink, M. Viergever (Eds.), *Scale-Space Theory in Computer Vision*, Lecture Notes in Computer Science, Vol. 1252, Springer, Berlin, 1997.
5. B. Jawerth, P. Lin, E. Sinzinger, *Lattice Boltzmann models for anisotropic diffusion of images*, J. Math. Imag. Vision, Vol. 11, 231–237, 1999.
6. B. Jähne, *Performance characteristics of low-level motion estimators in spatiotemporal images*, W. Förstner (Ed.), DAGM-Workshop Performance Characteristics and Quality of Computer Vision Algorithms, Braunschweig, September 18, 1997.
7. B. Jähne, H. Scharr, S. Körkel, *Principles of Filter Design*, B. Jähne, H. Haußecker, P. Geißler (Eds.), Handbook on Computer Vision and Applications, Vol. 2: Signal Processing and Pattern Recognition, Academic Press, San Diego, 125–152, 1999.
8. M. Nielsen, P. Johansen, O.F. Olsen, J. Weickert (Eds.), *Scale-Space Theories in Computer Vision*, Lecture Notes in Computer Science, Springer, Berlin, Vol. 1682, 1999.
9. T. Preußer, M. Rumpf, *An adaptive finite element method for large scale image processing*, J. Visual Comm. Image Repr., Vol. 11, 183–195, 2000.
10. H. Scharr, S. Körkel, B. Jähne, *Numerische Isotropieoptimierung von FIR-Filtern mittels Querglättung*, E. Paulus, F.M. Wahl (Eds.), Mustererkennung 1997, 367–374, Braunschweig, Springer, 1997.
11. H. Scharr, *Optimal Operators in Digital Image Processing*, PhD thesis, Interdisciplinary Center for Scientific Computing, University of Heidelberg, Germany, 2000.
12. J. Weickert, *Anisotropic Diffusion in Image Processing*, Teubner, Stuttgart, 1998.
13. J. Weickert, *Nonlinear diffusion filtering*, B. Jähne, H. Haußecker, P. Geißler (Eds.), Handbook on Computer Vision and Applications, Vol. 2: Signal Processing and Pattern Recognition, Academic Press, San Diego, 423–450, 1999.
14. J. Weickert, *Coherence-enhancing diffusion filtering*, Int. J. Comput. Vision, Vol. 31, 111–127, 1999.
15. J. Weickert, H. Scharr, *A scheme for coherence-enhancing diffusion filtering with optimized rotation invariance*, Report 4/2000, Computer Science Series, Dept. of Mathematics and Computer Science, University of Mannheim, Germany, 2000. To appear in J. Visual Comm. Image Repr.